

Lighting Up Fluorescent Silver Clusters via Target-Catalyzed Hairpin Assembly for Amplified Biosensing

Min Pan,[‡] Meijuan Liang,[‡] Junlin Sun, Xiaoqing Liu and Fuan Wang**

Key Laboratory of Analytical Chemistry for Biology and Medicine (Ministry of Education), College of Chemistry and Molecular Sciences, Wuhan University, Wuhan, Hubei, 430072, P. R. China

Corresponding authors

*E-mail: xiaoqingliu@whu.edu.cn

*E-mail: fuanwang@whu.edu.cn

Table of Contents

Table S1. The DNA/RNA sequences used to construct the amplified sensing platform.....	S-3
Table S2. Summary of the present enzyme-free AgNCs-based sensing platforms	S-4
Figure S1. Effect of CHA hairpin constitutes on AgNCs	S-5
Figure S2. Demonstration of the G-rich sequence-mediated lighting up AgNCs	S-6
Figure S3. CHA lighting up AgNCs by mutant hairpin monomers.....	S-8
Figure S4. Comparison of the non-amplified and amplified CHA-AgNCs systems	S-10
Figure S5. AFM characterization of the CHA-generated AgNCs	S-12
Figure S6. UV-vis absorption spectrum of the CHA-generated AgNCs	S-13
Figure S7. Fluorescence stability of the CHA-generated AgNCs	S-14
Figure S8. Traditional stoichiometric AgNCs-lighting up strategy for DNA assay	S-15
Figure S9. Optimization of reaction time for generalized miR-21 assay.....	S-16
Figure S10. Selectivity of the updated miR-21-targeting CHA-AgNCs system	S-18
References	S-20

Table S1. The DNA/RNA sequences used to construct the amplified sensing platform

No.	Sequence (5'→3')
H₁	GTT AAT GAC CTT CGT TAA TAG ACC GCT TGA TTT GAG GTC TAT TAA CGA AGG GGT GGG GTG GGG TGG G
H₂	ATT CTA GCA TGA AAA TAG ACC TCA AAT CAA GCG GTC TAT TAA CGA AGG GCT TGA TTT GA
H_{1T}	GTT AAT GAC CTT CGT TAA TAG ACC GCT TGA TTT GAG GTC TAT TAA CT ₂₁
H_{2T}	T ₁₄ ATA GAC CTC AAA TCA AGC GGT CTA TTA ACG AAG GGC TTG ATT TGA
H₃	CAG ACT GAT GTT GAG TGG TCT ATT AAC GAA GGT CAT TAA CTC AAC ATC AGT CTG ATA AGC TA
I	GGT CTA TTA ACG AAG GTC ATT AAC
P	CCC TTA ATC CCC TAT TTC ATG CTA GAA T
E	ATT CTA GCA TGA AAG AAG GGG TGG GGT GGG GTG GG
I_C	ATT CTA GCA TGA AAC GTT AAT AGA CC
I_G	GTT AAT GAC CTT AAG GGG TGG GGT GGG GTG GG
miR-21	UAG CUU AUC AGA CUG AUG UUG A
miR-122	GUU UGU GGU AAC AGU GUG AGG U
son DNA	ACU CCC AGA UGU UAG CAA C
β-actin mRNA	GCA AGC CAU GUA CGU UGC UAU CCA GGC UGU GCU AUC CCU GU

Table S2. Summary of the present enzyme-free AgNCs-based sensing platforms

System	Analyte	Linear range (nM)	Sensitivity (nM)	Ref.
Photo-induced electron transfer between G-quadruplex and DNA-AgNCs	DNA	1 ~ 100	0.6	1
FRET between graphene oxide and DNA-AgNCs	DNA	0 ~ 200	0.5	2
DNA-AgNCs-based molecular beacons	DNA	1 ~ 2000	25	3
Hybridization chain reaction-mediated DNA-AgNCs release from graphene oxide surface	DNA	10 ~ 100	1.18	4
Target-induced conformation changes of DNA-AgNCs	miRNA	0 ~ 1500	200	5
Construction of DNA-AgNCs through uncaging of DNA hairpin probe	miRNA	5 ~ 125	1.7	6
Strand displacement of DNA-AgNCs-decorated hairpin probe	miRNA	0 ~ 2500	100	7
Catalytic hairpin assembly enables the lighting up of DNA-AgNCs	DNA	0.5 ~ 15	0.02	This work
	miRNA	0.75 ~ 15	0.038	

Effect of CHA hairpin constitutes on AgNCs

In order to investigate the influence of CHA hairpin reactants on intrinsic AgNCs, the AgNCs probe (**P**) was incubated with CHA-hairpins **H**₁ and **H**₂, respectively. As compared with the intact AgNCs, no obvious fluorescence change of the AgNCs was observed when the AgNCs probe (**P**) was introduced into one of the CHA reactants (**H**₁ or **H**₂) (**Figure S1**). These results clearly demonstrate that the individual hairpin constitute of CHA circuit has no undesired side effect on the fluorescence of our AgNCs probe **P**.

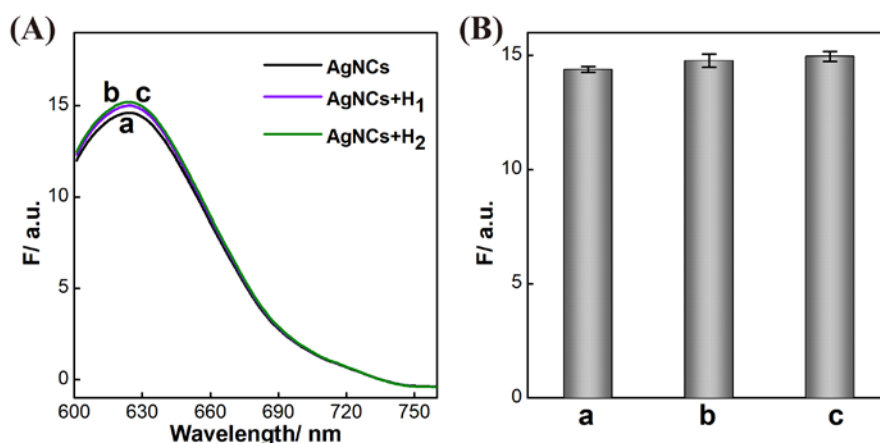


Figure S1. (A) Fluorescence spectra of the intact AgNCs (a) that was incubated with CHA constitute **H**₁ (b) or **H**₂ (c), respectively. (B) Summary of fluorescence results (at $\lambda=630$ nm) as shown in (A). The mixture consisting of analyte **I** (20 nM), AgNCs probe **P** (1 μ M) and CHA reactant **H**₁ or **H**₂ (500 nM) was carried out in reaction buffer (10 mM PB, 200 mM NaNO₃, 5 mM Mg(NO₃)₂, pH 7.0) for a fixed time interval of 2 h.

Demonstration of the G-rich sequence-mediated lighting up AgNCs

It was reported that the G-rich sequences could enhance the fluorescence of a specific AgNCs.⁸ The integration of CHA amplifier and G-rich sequence-mediated lighting up AgNCs still remains unexplored. After demonstrating the robustness of AgNCs to CHA amplifier reactants, the effectiveness of the G-rich enhancer sequence on AgNCs needs to be explored. Thus, an AgNCs enhancer sequence (E) consisting of a G-rich domain d and an anchoring domain e* was designed and incubated with the AgNCs probe (P) to assemble P-E complex. Then the low fluorescent AgNCs and G-rich sequences could be brought into close proximity through e-e* hybridization for lighting up AgNCs. Indeed, a dramatically enhanced fluorescence ($\lambda_{\text{max}} = 630 \text{ nm}$) was observed and visualized when the AgNCs probe P was incubated with AgNCs enhancer sequence E (**Figure S2**). The resulting red-emitting AgNCs could be visualized and discriminated easily from their control without enhancer sequence E (**Figure S2** inset). This implies that the AgNCs used in this study can be lightened up by G-rich sequence, which is consistent with previous literature.⁸

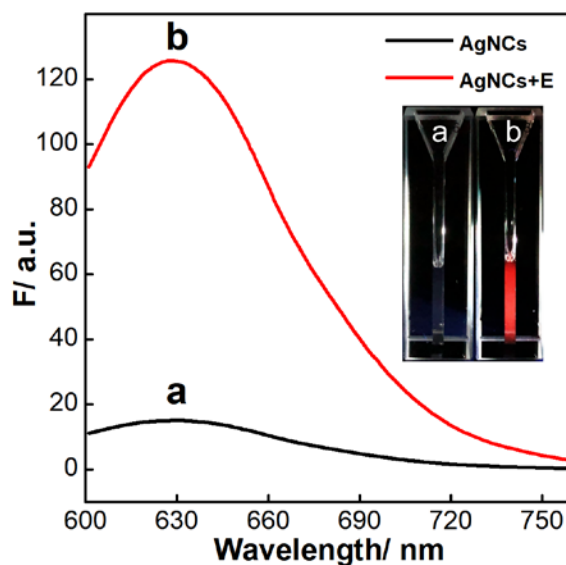


Figure S2. Fluorescence spectra of the AgNCs probe **P** before (a) and after (b) its incubation with AgNCs-enhancer sequence **E**. Inset: The lightening up photograph of the intact AgNCs (a) and the red-emitting fluorescent **P-E** complex (b) under visible and UV light. The images of these AgNCs samples were acquired by a digital camera and presented here without any contrast/color adjustment. The mixture consisting of **P** or **P+E** (20 nM **E**, 1 μ M of **P**) was carried out in reaction buffer (10 mM PB, 200 mM NaNO₃, pH 7.0) for a fixed time interval of 1 h.

CHA lighting up AgNCs by mutant hairpin monomers

To demonstrate the conjugation of CHA amplifier with AgNCs-lighting up strategy, one of the key hairpin components of CHA circuit (**H₁** or **H₂**) were substituted. As shown in **Figure S3A**, the newly introduced **H_{1T}** and **H_{2T}** are constructed by replacing the G-rich domain d of **H₁** and the capture domain e* of **H₂** with poly (T) fragments, respectively. Accordingly, the **H_{1T}-H₂**, **H₁-H_{2T}** and **H_{1T}-H_{2T}** pairs were incubated with DNA analyte **I** (15 nM) to investigate the integration of CHA amplifier with AgNCs-lighting up strategy. As expected, no fluorescence enhancement was observed for the initiator-triggered CHA system as the AgNCs and G-rich enhancer could not be brought into close proximity for **H_{1T}-H₂**, **H₁-H_{2T}** and **H_{1T}-H_{2T}** mixtures as compared with the background fluorescence signal (Figure S3). Thus, an apparent transformation from low fluorescent AgNCs to bright red-emitting AgNCs was achieved through firmly connection of G-rich sequence with intact AgNCs. This, on the other side, demonstrated the successful conjugation between CHA-amplifier and AgNCs-lighting up strategy.

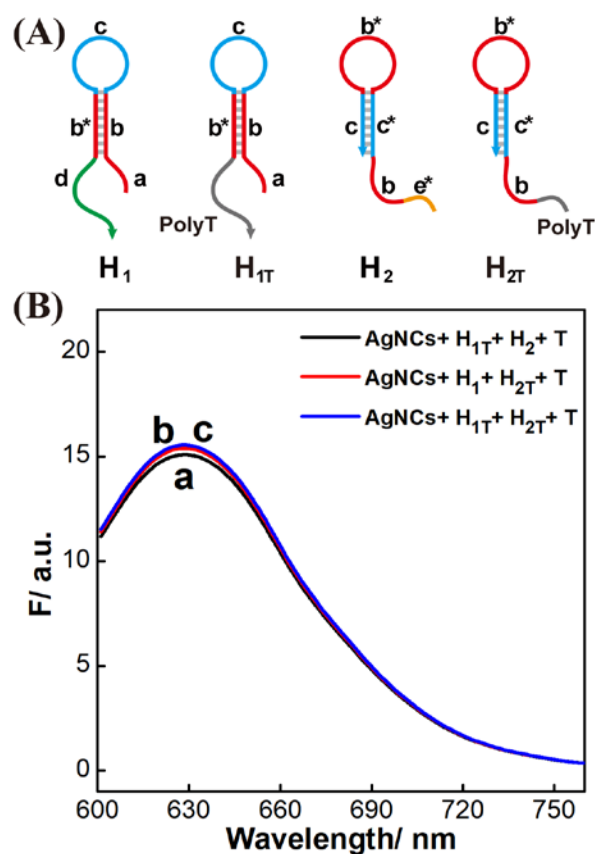


Figure S3. (A) Schematically illustration of the structures of control hairpin probes that got involved in the CHA-circuit. (B) Fluorescence spectra of the AgNCs probe **P** incubated with CHA-mediated autonomous cross-hybridization of H_{1T} - H_2 (a), H_1 - H_{2T} (b) and H_{1T} - H_{2T} (c) pairs. The mixture consisting of **P** (1 μ M), analyte (**I**, 15 nM) and the corresponding hairpin reactants (500 nM each), was carried out in reaction buffer (10 mM PB, 200 mM NaNO_3 , 5 mM $\text{Mg}(\text{NO}_3)_2$, pH 7.0) for a fixed time interval of 2 h.

Comparison of the non-amplified and amplified CHA-AgNCs systems

To demonstrating the signal amplification capacity of the CHA-amplifier, a traditional stoichiometric G-rich enhancement scheme (nominated as non-amplified system) was designed as an important control, **Figure S4A**. The capture subunit **I_C** was constructed to include AgNCs-capturing domain e* and a recognition domain b. And the enhancer subunit **I_G** was engineered to have AgNCs-lighting domain d and the other recognition domain a. Then the same DNA analyte **I** can hybridize with both of **I_C** and **I_G** subunits and connect the AgNCs-capturing sequence e* and G-rich enhancer sequence d. The resulting **I-I_C-I_G** complex could further capture AgNCs through its incubation with the AgNCs probe **P**, resulting in bright red-emitting AgNCs. For the comparison of present CHA-amplified system with conventional non-amplified system, the CHA-AgNCs system consisting of the AgNCs probe **P** (1 μ M), DNA analyte (**I**, 10 nM) and **H₁+H₂** mixture (500 nM each), and the traditional control system consisting of the AgNCs probe (**P**, 1 μ M), DNA analyte (**I**, 10 nM) and **I_C+I_G** mixture (500 nM each) were respectively carried out in reaction buffer (10 mM PB, 200 mM NaNO₃, 5 mM Mg(NO₃)₂, pH 7.0) for a fixed time interval of 2 h. Clearly, a nearly 10-fold higher of fluorescence response over traditional system (**Figure S4B** and **S4C**) was acquired, revealing an enhanced signal response of the present CHA amplifier ($\Delta F/F_0 = 2.81$) over non-amplifier ($\Delta F/F_0 = 0.28$).

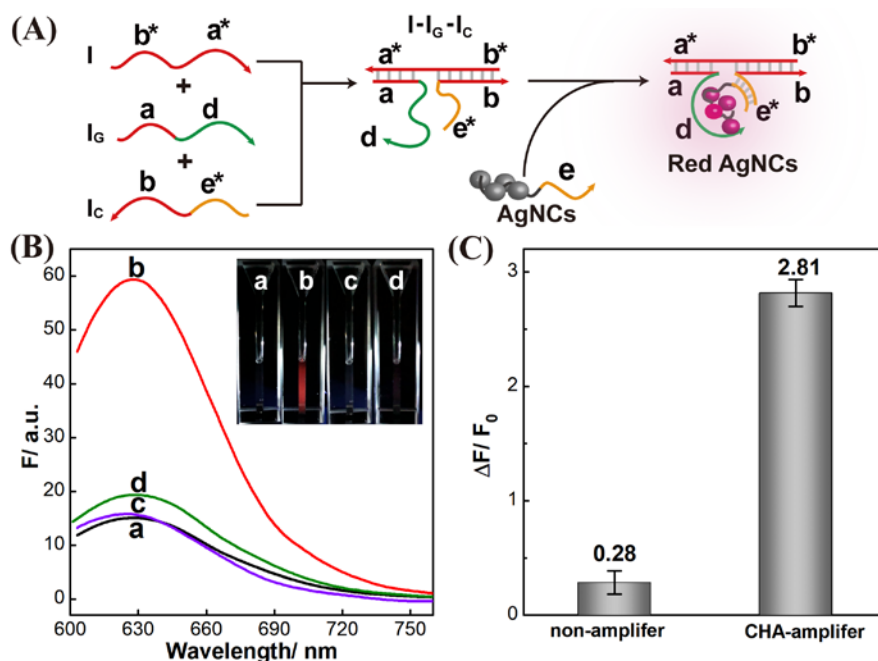


Figure S4. (A) Principle of the non-amplified analyte (**I**) sensing by traditional stoichiometric G-rich enhancement without signal amplification strategy (nominated as non-amplified system). (B) Fluorescence spectra generated by the CHA-amplified AgNCs system shown in **Figure 1A** (a: without **I**; b: with 10 nM **I**) and the non-amplified system shown in **Figure S4A** (a: without **I**; b: with 10 nM **I**), respectively. (C) Summary of the fluorescence spectra shown in (B). Here the fluorescence intensity was acquired at a fixed wavelength of 630 nm. F_0 represents the original fluorescence intensity and error bars are derived from $n = 5$ experiments.

AFM characterization of the CHA-generated AgNCs

AgNCs was chemically synthesized by NaBH_4 -mediated reduction of Ag precursor (AgNO_3) *via* an engineered DNA template. The assembled \mathbf{H}_1 - \mathbf{H}_2 duplex of CHA reaction then captures the functionalized low fluorescent DNA-AgNCs probe (\mathbf{P}) through e/e* duplex shown in **Figure 1A**, resulting in fluorescent bright red-emitting AgNCs. The generated AgNCs was then imaged by AFM, **Figure S5**. The assembled CHA-AgNCs complexes show highly ordered stripes over the entire surface (**Figure S5A**). In particular, the pitch of the stripes is measured to be ~ 2 nm (**Figure S5B**), which is consistent with the typical height of AgNCs.⁹

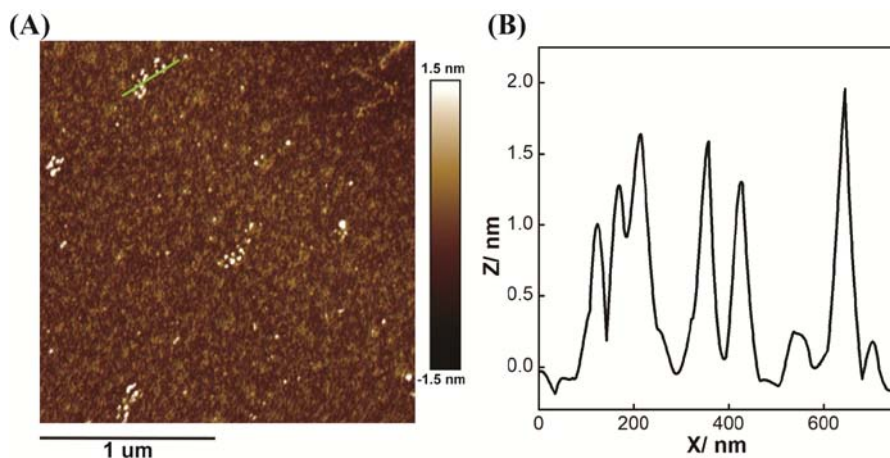


Figure S5. (A) AFM characterization of the AgNCs of CHA-AgNCs system. (B) Cross-section analysis of the assembled AgNCs (corresponding to the green line of A). The mixture consisting of \mathbf{H}_1 + \mathbf{H}_2 + \mathbf{P} (500 nM of hairpins, 1 μM of \mathbf{P} and 20 nM of analyte \mathbf{I}) was carried out in reaction buffer for a fixed time interval of 2 h. The CHA-generated CHA-AgNCs complex was diluted and deposited on a freshly prepared mica for AFM characterization.

UV-vis absorption spectrum of the CHA-generated AgNCs

The functionalized low fluorescent DNA-AgNCs probe (**P**) was lighted up through the CHA duplex, resulting in bright red-emitting fluorescent AgNCs. The UV-vis absorption spectrum of the generated fluorescent AgNCs was then investigated, **Figure S6**. The assembled CHA-AgNCs show absorption from 500 nm to 600 nm which is consistent with the excitation wavelength ($\lambda_{\text{max}}=580$ nm).

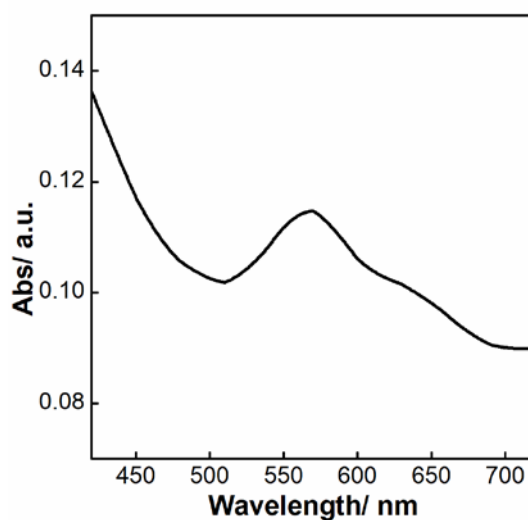


Figure S6. UV-vis spectrum of the AgNCs as generated from the CHA-AgNCs system. The CHA-AgNCs mixture, consisting of CHA hairpins (500 nM each), DNA analyte (**I**, 100 nM) and AgNCs probe (**P**, 1 μ M), was carried out in PB (10 mM, containing 200 mM of NaNO_3 and 5 mM of $\text{Mg}(\text{NO}_3)_2$) at pH=7.0 for a fixed time interval of 2 h.

Fluorescence stability of the CHA-generated AgNCs

The stability of the DNA-AgNCs is of vital importance in the sensing performance. To get a more reliable fluorescence probe, the fluorescence stability of DNA-AgNCs was investigated (**Figure S7**). After 4h, the decrease of the fluorescence intensity of DNA-AgNCs was negligible. The fluorescent DNA-AgNCs was stable enough for the sensing process.

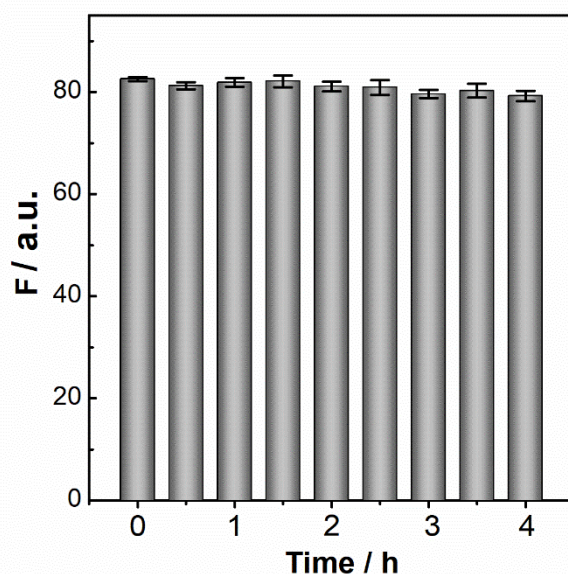


Figure S7. Stability investigation of the CHA-generated fluorescent AgNCs. The CHA-AgNCs mixture, consisting of CHA hairpins (500 nM each), DNA analyte (I, 100 nM) and AgNCs probe (P, 1 μ M), was carried out in PB (10 mM, containing 200 mM of NaNO_3 and 5 mM of $\text{Mg}(\text{NO}_3)_2$) at pH=7.0 for 2 h. The fluorescence intensity of the DNA-AgNCs (at $\lambda = 630$ nm) was collected every 30 min during the sensing process.

Traditional stoichiometric AgNCs-lighting up strategy for DNA assay

The traditional stoichiometric AgNCs-lighting up system shown in **Figure S5A** was denoted as non-amplified control system and applied for analyzing the same analyte **I** of varied concentrations under the same environment as CHA-amplified AgNCs system, **Figure S8**. The fluorescence of AgNCs intensified with increasing concentrations of **I**, demonstrating the universal applicability of the present non-amplified AgNCs-lighting up system. The detection limit of the non-amplified system corresponds to 450 pM, which is much higher than that of CHA-amplified AgNCs system. This, on the other hand, demonstrates the satisfactory signal amplification of our proposed CHA-AgNCs system shown in **Figure 1A**.

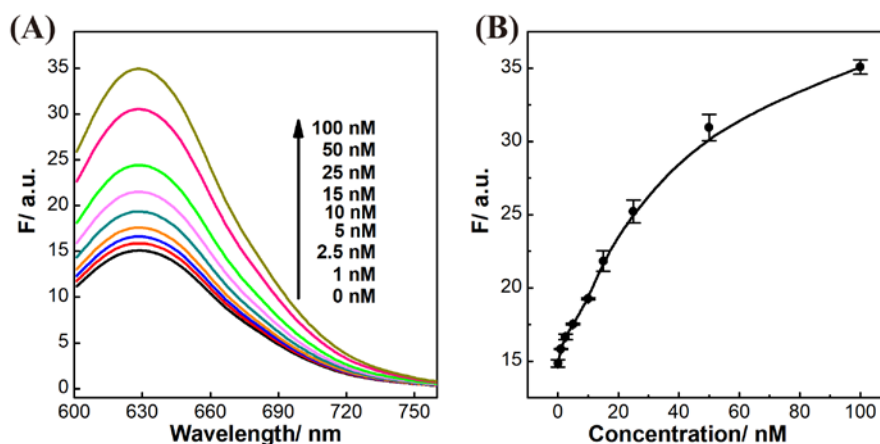


Figure S8. Traditional stoichiometric AgNCs-lighting up system upon analyzing different concentrations of target DNA. The fluorescence spectra (**A**) and the corresponding calibration curve (**B**) of the non-amplified AgNCs system, consisting of $I_C + I_G + P$ mixture (500 nM of I_C or I_G , 1 μ M of **P**) and different concentrations of analyte **I**, was carried out in reaction buffer (10 mM PB, 200 mM $NaNO_3$, 5 mM $Mg(NO_3)_2$, pH 7.0) for a fixed time interval of 2 h. Error bars were derived from $n = 5$ experiments.

Optimization of reaction time for generalized miR-21 assay

The present isothermal CHA-lighting up AgNCs system represents an optimized sensing platform. It can be easily adapted to analyze other nucleic acid targets without further significant optimization of the established system. This was exemplified with the amplified microRNA assay by using microRNA-21 (miR-21) as the model target. A “helper” hairpin **H₃** was introduced to recognize and hybridize with miR-21. Then the opened **H₃** motivated the sequential cross-hybridizations of CHA hairpins, resulting in the assembly of **H₁-H₂** duplex and then the AgNCs lighting up. **Figure S9** shows time-dependent fluorescence changes of the updated CHA-AgNCs system with and without miR-21 target. Scarcely no fluorescence change was observed for the updated CHA-AgNCs system without miR-21 target, indicating that the helper hairpin **H₃** of sensing module is stable enough to eliminate false signal leakage. However, a significant increasement of fluorescence intensity was observed for miR-21-triggered CHA-AgNCs system and it leveled off after 80 min, which is attributed to an efficient formation of CHA-generated red-emitting AgNCs. Accordingly, the optimal reaction time is chosen 80 min for all of the subsequent miR-21 experiment.

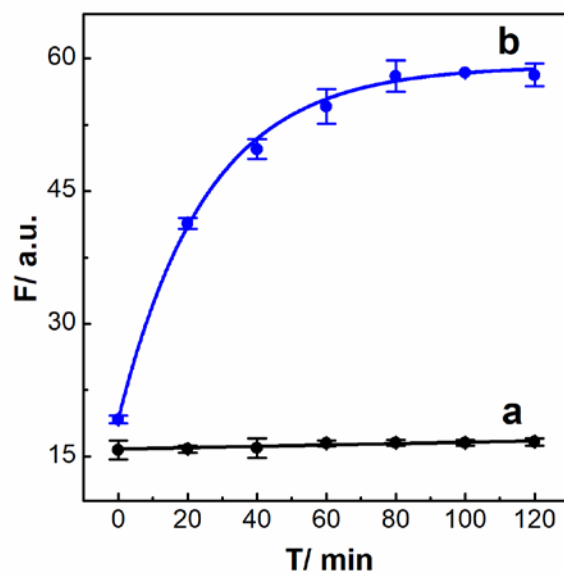


Figure S9. Time-dependent fluorescence changes of the updated CHA-mediated lighting up AgNCs ($\lambda = 630$ nm) shown in **Figure 3A** without (a) and with (b) miR-21 (40 nM). The updated CHA-AgNCs system consisting of $\mathbf{H}_1 + \mathbf{H}_2 + \mathbf{H}_3 + \mathbf{P}$ mixture (\mathbf{H}_1 : 200 nM; \mathbf{H}_2 : 200 nM; \mathbf{H}_3 : 50 nM, \mathbf{P} : 1 μ M) was carried out in reaction buffer with varied reaction time. Error bars were derived from $n = 5$ experiments.

Selectivity of the updated miR-21-targeting CHA-AgNCs system

As an important prerequisite parameter, the selectivity of the present CHA-AgNCs system needs to be investigated for clinical application purpose. **Figure S10** depicts the fluorescence response upon analyzing 15 nM of miR-21 and its interfering nucleic acids: β -actin mRNA, son DNA and miR-122. Obviously, the fluorescence intensities generated by the different interfering nucleic acids (curve b, c and d, respectively) are almost the same with the background signal (curve a) of the updated CHA-AgNCs system (without analyte). A comparably dramatically enhanced fluorescence spectrum was observed upon analysing miR-21 (curve e) under the same conditions. This signal difference of fluorescence can be visualized and discriminated easily from its interfering nucleic acids, providing a facile way for accurate microRNA assay. It is clear that only the miR-21-motivated CHA-AgNCs system could generate a bright red-emitting AgNCs readout signal. All of the other interfering RNAs could not induce obvious fluorescence signals of AgNCs. The present CHA-lighting up AgNCs sensing platform possessed high selectivity and might discriminate the target microRNA from its biological interference sequences.

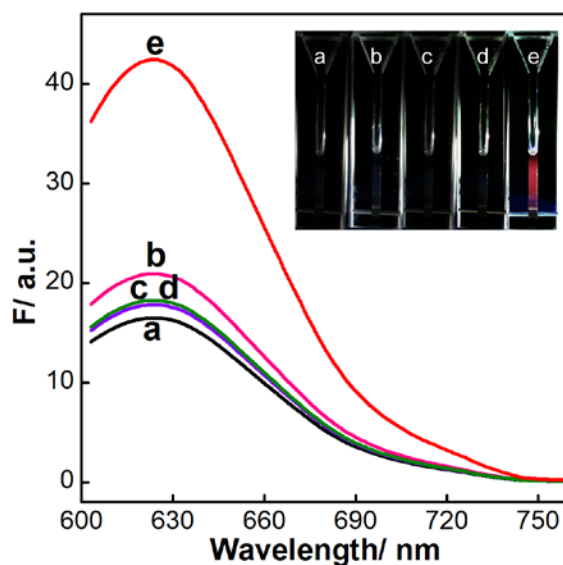


Figure S10. Fluorescence spectra generated by the updated CHA-AgNCs system upon analyzing different analyte: (a) no analyte; (b) β -actin; (c) miR-122; (d) son DNA and (e) miR-21. Inset: The photograph of CHA-AgNCs system was obtained upon analyzing different analytes under UV light ($\lambda=365$ nm). The image was acquired by a digital camera and presented here without any contrast/color adjustment. The $\mathbf{H_1+H_2+H_3+P}$ mixture ($\mathbf{H_1}$: 200 nM; $\mathbf{H_2}$: 200 nM; $\mathbf{H_3}$: 50 nM, \mathbf{P} : 1 μ M) was incubated with different analytes (15 nM each) in reaction buffer for a fixed time interval of 80 min.

References

- (1) Zhang, L.; Zhu, J.; Guo, S.; Li, T.; Li, J.; Wang, E. Photoinduced Electron Transfer of DNA/Ag Nanoclusters Modulated by G-Quadruplex/Hemin Complex for the Construction of Versatile Biosensors. *J. Am. Chem. Soc.* **2013**, *135*, 2403-2406.
- (2) Liu, X.; Wang, F.; Aizen, R.; Yehezkeli, O.; Willner, I. Graphene Oxide/Nucleic-Acid-Stabilized Silver Nanoclusters: Functional Hybrid Materials for Optical Aptamer Sensing and Multiplexed Analysis of Pathogenic DNAs. *J. Am. Chem. Soc.* **2013**, *135*, 11832-11839.
- (3) Zhang, Y.; Zhu, C.; Zhang, L.; Tan, C.; Yang, J.; Chen, B.; Wang, L.; Zhang, H. DNA-Templated Silver Nanoclusters for Multiplexed Fluorescent DNA Detection. *Small* **2014**, *11*, 1385-1389.
- (4) Zhang, S.; Wang, K.; Li, K.-B.; Shi, W.; Jia, W.-P.; Chen, X.; Sun, T.; Han, D.-M. A DNA-Stabilized Silver Nanoclusters/Graphene Oxide-Based Platform for the Sensitive Detection of DNA through Hybridization Chain Reaction. *Biosens. Bioelectron.* **2017**, *91*, 374-379.
- (5) Yang, S. W.; Vosch, T. Rapid Detection of MicroRNA by a Silver Nanocluster DNA Probe. *Anal. Chem.* **2011**, *83*, 6935-6939.
- (6) Xia, X.; Hao, Y.; Hu, S.; Wang, J. Hairpin DNA Probe with 5'-TCC/CCC-3' Overhangs for the Creation of Silver Nanoclusters and miRNA Assay. *Biosens. Bioelectron.* **2014**, *51*, 36-39.
- (7) Zhang, J.; Li, C.; Zhi, X.; Ramón, G. A.; Liu, Y.; Zhang, C.; Pan, F.; Cui, D. Hairpin DNA-Templated Silver Nanoclusters as Novel Beacons in Strand Displacement Amplification for MicroRNA Detection. *Anal. Chem.* **2016**, *88*, 1294-1302.
- (8) Yeh, H.-C.; Sharma, J.; Han, J. J.; Martinez, J. S.; Werner, J. H. A DNA-Silver Nanocluster Probe That Fluoresces upon Hybridization. *Nano Lett.* **2010**, *10*, 3106-3110.
- (9) Dong, H.; Hao, K.; Tian, Y.; Jin, S.; Lu, H.; Zhou, S.-F.; Zhang, X. Label-Free and Ultrasensitive microRNA Detection Based on Novel Molecular Beacon Binding Readout and Target Recycling Amplification. *Biosens. Bioelectron.* **2014**, *53*, 377-383.